sciendo

ACTA CHEMICA IASI, **26_2**, 249-262 (2018)

DOI: 10.2478/achi-2018-0016

MAGNETIC AND ANTIBACTERIAL STUDIES OF NANOFERRITES PREPARED BY SELF PROPAGATING HIGH-TEMPERATURE SYNTHESIS ROUTE

Ravi C. Bharamagoudar[a], Anil S. Patil[b], Shridhar N. Mathad[c*], Vijay M. Kumbar[d], Laxmi B. Kankanawadi[e]

[a]*Department of Physics, Jain College of Engineering, Belagavi, India*

[b]*KLE Dr. M. S. Sheshgiri College of Engineering and Technology, Belagavi*

[c]*Department of Physics, KLEIT, Hubballi, India*

[d]*Maratha Mandal's, Central Research Laboratory, Belagavi, India*

[e]*Hirashugar Institute of Technology, Nidasoshi.Belagavi, India*

Abstract: The main objective of the manuscript is the structural analysis, magnetic investigation and antimicrobial activity of $Mn_{1-x}Zn_xFe_2O_4$ with stoichiometry (x = 0, 0.25, 0.5, 0.75, and 1.0). The Mn-Zn nanoferrites were synthesized by self propagating high-temperature synthesis using a mixture of fuels. The synthesized Mn-Zn nanoferrites were characterized by X-ray diffraction (XRD) that confirms cubic crystal structure with lattice constant in the range 8.372-8.432A^o. It is observed that saturation magnetization (Ms), remanence magnetization (Mr) and magneton number (Mr/Ms) decreased gradually with the increasing of Zn^{2+} concentration. The decrease in the saturation magnetization may be explained as, the Zn^{2+} concentration increases, the relative number of ferric ions on the A sites diminishes and this reduces the A–B interaction. Further, the synthesized Mn-Zn nanoferrites were tested for antibacterial activities against two-gram positive strains (*Staphylococcus aureus* ATCC No–12598,

* Shridhar N. Mathad, *e-mail:* physicssiddu@gmail.com

Lactobacillus amylovorus ATCC No– 12598), gram-negative strains *E.coli* ATCC No – 25922, *Pseudomonas*- ATCC No- 25619) and one fungal strain (*C.albicans* - ATCC No – 2091).

***Keywords*:** $Mn_{1-x}Zn_xFe_2O_4$, Ferrites, XRD, antimicrobial activity.

Introduction

The ferromagnetic or ferrimagnetic materials are those which are strongly attracted to a magnet and can be easily magnetized. These include iron, nickel, cobalt and some alloys of rare-earth metals etc. Ferrimagnetic materials are mainly composed of oxides of iron and other suitable metal oxides, called as ferrites. Ferrites exhibit semiconducting nature, possess high electrical resistivity, low eddy current, dielectric losses, high saturation magnetization, high permeability and moderate permittivity. Magnetic material synthesis methodology plays vital role, that realize its applications altogether fields.[1-2] Ferrites are comprehensively employed in radar, audio–video and digital recording, bubble devices, memory cores of computers, satellite communication and microwave devices.[1-4] Ferrites are classified into three classes based on their crystal structures as spinel ferrite, garnet and hexagonal ferrite. Spinel is the most widely used family of ferrites. High value of electrical resistivity and low eddy current losses make them ideal for their use at microwave frequencies as Microwave component (rotator, isolator). The spinel class of ferrite materials are technologically important due to their novel applications in various fields like medicine, gas sensing, catalysis, magnetic tape recording and miniaturization of electronic components like transformer, inductor etc. Spinel ferrites are also used in the field of engineering viz. telecommunication, microwave and electronics.[5-8]

These spinel ferrites have general chemical formula of MFe_2O_4, where M can be any divalent ion of metals such as nickel (Ni^{2+}), cadmium (Cd^{2+}), zinc (Zn^{2+}), magnesium (Mg^{2+}) and copper (Cu^{2+}) or trivalent ion of metals like aluminium (Al^{3+}), chromium (Cr^{3+}).[9-16] Spinel ferrites have the spinel cubic structure, complex in nature and consist of eight formula units of MFe_2O_4. A typical example of spinel ferrite is $ZnFe_2O_4$, $MgFe_2O_4$ and $MnFe_2O_4$. Magnetic nanoparticles of spinel ferrites have smaller size and larger surface area leading to greater chemical reactivity. Surface effects of nano-materials can become more predominant in determining the material properties, leading to novel microstructure, optical, electrical, dielectric and magnetic properties. Consequently, the ferrites in nanocrystalline form find applications in recent fields like magnetically guided drug delivery, magnetic resonance imaging (MRI), sensors (humidity and gas), magnetic fluids, etc.[17-20] In the environmental science, ferrite nanoparticles are used in treating polluted waste water from industry. The recent applications also include high density information storage, ferro fluids, catalyst, sensors, etc.[21] The ferrites have been developed by using different methods such as ball milling method,[22] co-precipitation method,[23] hydrothermal method[24] and auto combustion method.[25] Among these methods, the solution combustion method is a facile approach with great economic and technical advantages to obtain highly crystalline nanoparticles.

In the present investigation we adopted the solution combustion method to synthesize $Mn_{1-x}Zn_xFe_2O_4$ (x = 0, 0.25, 0.5, 0.75, and 1.0) nanoferrite particles using urea and glucose as a mixed fuels. Furthermore, their structural studies were realized by XRD and their magnetic behavior was studied using vibrating sample magnetometer (VSM). The antibacterial activity of the synthesized ferrites was evaluated against two gram positive

strains (*Staphylococcus aureus* ATCC No–12598, *Lactobacillus amylovorus* ATCC No – 12598), two gram-negative strains (*E. coli* ATCC No – 25922, *Pseudomonas* ATCC No – 25619) and one fungal strain (*C. albicans* ATCC No – 2091).

Experimental

Chemistry

Nanocrystalline $Mn_{1-x}Zn_xFe_2O_4$ (x = 0, 0.25, 0.5, 0.75, and 1.0) ferrites have been prepared by self propagating high temperature synthesis using glucose and urea with O/F ratio equal to one. Manganese nitrate [$Mn(NO_3)_2 \cdot 6H_2O$], zinc nitrate [$Zn(NO_3)_2 \cdot 6H_2O$] and iron nitrate [$Fe(NO_3)_3 \cdot 9H_2O$] have been homogeneously mixed with urea [$CO(NH_2)_2$] and glucose [$C_6H_{12}O_6$] using distilled water. The aqueous solution containing the redox mixture have been taken in a Pyrex dish and heated in a muffle furnace maintained at 450 ± 10°C. Initially, the solution boils froths and ignites to yield fine particles of Mn-Zn nanoferrites. The whole preparation process has been completed within 20 minutes, whereas the reaction time of the actual ignition was less than 5s.

Biological assays

Ciprofloxacin and fluconazole were used as standard antibacterial and antifungal agents.

a) Determination of Minimum Inhibitory Concentration (MIC)

The MIC of nanoparticles was determined by broth dilution in accordance with BMD guidelines as described by the Clinical and Laboratory Standards Institute (CLSI).[1-2] Briefly, 24h bacteria cultures were diluted in fresh BHI to achieve the turbidity of the 0.5 McFarland standards. Two-fold serial dilutions of nanoparticles (from 2500 µg/ml) in BHI culture

medium were added into micro centrifuge tubes. 2% Chlorhexidine gluconate was used as a positive control. Tubes were incubated 24 h at 37°C in aerobic condition. After the incubation bacterial growth was recorded visually. MIC values were determined as the lowest concentrations at which no bacterial growth occurred.

b) Determination of Minimum Bactericidal Concentration (MBC)

To determine the MBC values, aliquots (5 µl) of each well showing no visible growth were spread on sheep blood-supplemented BHI agar plates, and were incubated for 2 days at 37°C. The MBC values were determined as the lowest concentrations at which no colony formation occurred.[26-27]

Results and Discussion

XRD Analysis

The room temperature X-ray diffraction patterns of all the samples of $Mn_{1-x}Zn_xFe_2O_4$ nanoferrites are shown in Figure 1. The synthesized ferrite powder is characterized by X-ray diffractometer using Shimadzu 7000S with CuKα (Wavelength, λ=0.154056 nm) radiation in the 2θ range of 20° -80° at room temperature.

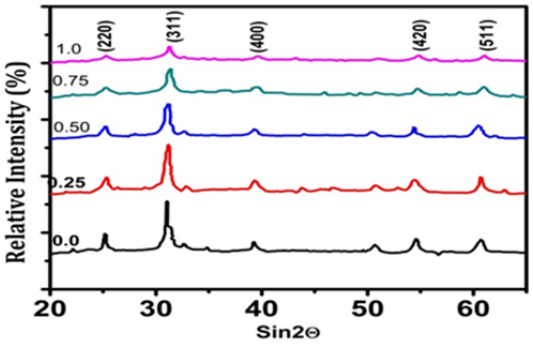

Figure 1. XRD pattern of synthesized $Mn_{(1-x)}Zn_xFe_2O_4$, where x= 0, 0.25, 0.5, 0.75 and 1.

The Powder XRD (PXRD) result confirms the formation of spinel cubic structure which matches with JCPDS No. 22-1012. The average

crystallite size of the each composition was calculated from line width of (311) peak of XRD pattern and 2θ which is around 34° using the Scherrer formula.[28] The average particle size is calculated to be 25 nm.

$$D = \frac{K \cdot \lambda}{\beta \cdot cos\theta} \quad (1)$$

where D is crystallite size, λ is wavelength of X-ray radiation, θ is Bragg's angle, β is full width at half maximum (FWHM). The lattice parameter varies as Zn^{2+} concentration increases and lies in the range 8.372-8.432 Å. The average particle size of all the composition varies in the range of 25 to 35 nm.

Magnetic Properties

Magnetization was carried out by vibrating sample magnetometer (VSM) mounted on an electromagnet with a bipolar source of maximum applied field of 1.5 T at room temperature. Magnetic hysteresis curves (M-H Curve) of the samples investigated at room temperature were shown in Figure 2. The narrow hysteresis loops were observed and hence synthesized materials are soft magnetic material. The data presented in Table 1, show that values of saturation magnetization (Ms), remanent magnetization (Mr), remanent ratio, coercivity (H_c) and magneton number (n_B) are found to be decreasing with increasing of Zn^{2+} concentration. The increase of Zn content, make the coercivity (H_c) values of samples low. Therefore, the probability of domain rotation is as well low, which are used for low core loss applications due to larger grain size. It evidences the super paramagnetic nature of Mn-Zn ferrites.[29] When zinc concentration (Zn^{2+}) increases, Fe^{3+} ions migrate from octahedral (B site) to tetrahedral (A site) and Mn^{2+} concentration decreases from both tetrahedral (A site) and octahedral (A site). Therefore, the magnetization of the B-site decreases

while that of A-site increases, which results in decrease of net magnetization. The ferrite nanoparticles of the series $Mn_{1-x}Zn_xFe_2O_4$ were found to be showing reduced magnetization.[30] Zinc ferrite is a normal spinel and has no magnetic moment. Non magnetic Zinc ion (Zn) is substituted for Manganese ferrite site, it has stronger preference for the tetrahedral site (A-site) than does the ferric ion and thus brings down the amount of Fe^{3+} ions on the A-site. Because of the antiferromagnetic coupling, the result is an increase in magnetic moment on the octahedral site (B-site) and an increase in the saturation magnetization.[30-31] The respective reduction in magnetization may be due to a rearrangement of cations because of the changed preferential occupancy in the case of nanosized ferrites causing change in distribution of Mn^{2+} and Zn^{2+} on the two sites.[31] Lesser magnitudes of magnetization and the presence of a net magnetic moment of the ferrite (Zn), due to zinc, signifies the presence of Zn^{2+} ions on the octahedral site.

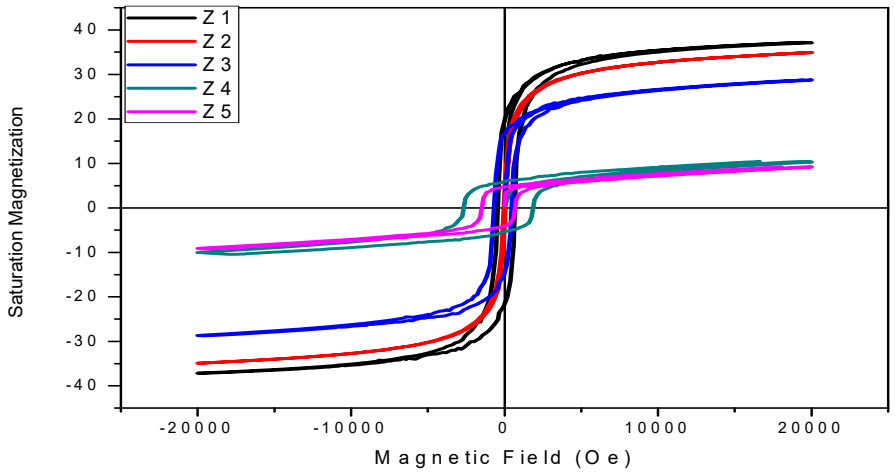

Figure 2. M-H loop of the synthesized $Mn_{(1-x)}Zn_xFe_2O_4$, where x= 0, 0.25, 0.5, 0.75 and 1.

Table 1. Magnetic properties of $Mn_{1-x}Zn_x Fe_2O_4$ nanoferrites at 300 K.

Composition (x)	Sample	Saturation Magnetization (M_s) Am^2/kg	Remanence magnetization (M_r)Am^2/kg	Coercivity (H_c) Tesla	Magneton number (nB)
0.00	Z1	71.75	29.11	0.0163	2.469
0.25	Z2	53.20	20.54	0.0166	1.824
0.50	Z3	50.67	21.46	0.0168	1.743
0.75	Z4	41.73	16.95	0.0164	1.435
1.00	Z5	10.73	4.349	0.0164	0.394

Antibacterial Studies

The antibacterial activities of Mn-Zn nanoferrites against two-gram positive strains (*Staphylococcus aureus* ATCC No–12598, *Lactobacillus amylovorus* ATCC No– 12598), two gram-negative strains (*E.coli* ATCC No – 25922, *Pseudomonas* ATCC No – 25619) and one fungal strain (*C.albicans* ATCC No – 2091).

The minimum inhibitory concentration (MIC) and minimum bactericidal concentration (MBC) of $MnFe_2O_4$ and $Mn_{0.75}$ $Zn_{0.25}Fe_2O_4$ against the test strains ranged from 1250 and 2500 µg/mL, respectively. Similarly the MIC and MBC of $Mn_{0.5}$ $Zn_{0.5}Fe_2O_4$ and $ZnFe_2O_4$ against the test strains showed in the range of 625µg/mL and 1250 µg/mL, respectively. Similarly, the MBCs of nanoparticles ranged from 1250-2500 µg/mL as shown in Table 2.

Table 2. MIC and MBC values of Nanoparticles against Bacterial and Fungal strains.

Nanoparticles	Micro-organisms	MIC (mg/mL)	MBC (mg/mL)
$MnFe_2O_4$	*Staphylococcus aureus*	1250	2500
	Lactobacillus amylovorus	1250	2500
	E. coli	1250	2500
	Pseudomonas aeruginosa	1250	2500
	Candida albicans	1250	2500
$Mn_{0.75}Zn_{0.25}Fe_2O_4$	*Staphylococcus aureus*	1250	2500
	Lactobacillus amylovorus	1250	2500
	E, coli	1250	2500
	Pseudomonas aeruginosa	1250	2500
	Candida albicans	1250	2500
$Mn_{0.5}Zn_{0.5}Fe_2O_4$	*Staphylococcus aureus*	1250	2500
	Lactobacillus amylovorus	625	1250
	E. coli	625	1250
	Pseudomonas aeruginosa	625	1250
	Candida albicans	625	1250
$Mn_{0.25}Zn_{0.75}Fe_2O_4$	*Staphylococcus aureus*	625	1250
	Lactobacillus amylovorus	625	1250
	E. coli	625	1250
	Pseudomonas aeruginosa	625	1250
	Candida albicans	625	1250
$ZnFe_2O_4$	*Staphylococcus aureus*	625	1250
	Lactobacillus amylovorus	625	1250
	E coli	625	1250
	Pseudomonas aeruginosa	1250	2500
	Candida albicans	625	1250

The antibacterial activity of metal oxides is due to a number of mechanisms, the metal nanoparticles are carrying the positive charges and the microbes are having the negative charges which create the electromagnetic attraction between the nanoparticles and the microbes. This leads to immediate death of microbes due to their oxidation. Metal complexes are toxic to some bacterial and fungal species at small concentration therefore some metals were used as antimicrobial agents since from ancient times. Another antimicrobial activity of metal oxides is the metal reduction potential. The mechanism is a main characteristic of metals

which involve in the redox reactions as catalytic co-factors cell enzymes thus generating reactive oxygen species (ROS). These species can causes an oxidative stress resulting in the damage of cellular proteins, lipids and DNA and increasing level of ROS further triggers pro-inflammatory signaling cascades into the cell able to induce its programmed death.

The metal donor atom selectivity and/or speciation mechanism is based on the fact that bacterial membranes contain macromolecules with highly electronegative chemical groups that serve as sites of adsorption for metal ions carrying the positive charges which exert bactericidal toxicity. Also, metal ions generally bind to some atoms of donor ligands, such as O, N and S, through strong and selective interactions. Thus, external metal ions or their complexes can replace original metals present in biomolecules leading to cellular dysfunction.[32-34] And the second reason is the presence of generated reactive oxygen species (ROS) that may lead to oxidative stress and lipid peroxidation causing oxidative DNA damage in the microbes.[26, 32-34] In conclusion, the metal nanoparticles interact with membrane proteins resulting in the damage of the bacterial membrane and the biological interaction of nanoparticles with macromolecules leading to inhibition of microbes growth.

Conclusion

We have successfully synthesized the nanocrystalline Mn–Zn ferrites by Self Propagating High-Temperature Synthesis method (combustion method). Spinal cubic structure was confirmed by XRD. The narrow hysteresis loops reveals that synthesized materials are soft magnetic material. The biological activity testes against *Staphylococcus aureus*, *Lactobacillus amylovorus*, *E. coli*, *Pseudomonas* and *C. albicans* showed

the nanoferrites $Mn_{0.25}Zn_{0.75}Fe_2O_4$ and $ZnFe_2O_4$ have a high antibacterial activity. Mn–Zn ferrites have high potentials to be used in biomedical and biotechnology applications.

References

1. Hagfeldth, A.; Gratzel, M. Light-induced redox reactions in nanocrystalline systems. *Chem. Rev*. **1995**, *95*, 49-68.

2. Goldman, A. *Modern Ferrite Technology*. Springer-Verlag: Pittsburgh, 2006.

3. Viswanathan, B., Murthy, V.R.K. *Ferrite Materials*. Springer Verlag: Berlin, 1990.

4. Prasad, S.; Gajbhiye, N.S. Magnetic studies of nanosized nickel ferrite particles synthesized by the citrate precursor technique. *J. Alloys Compd*. **1998**, *265*, 87-92.

5. Verma, A.; Goel, T.C.; Mendiratta, R.G.; Gupta, R.G. High-resistivity nickel–zinc ferrites by the citrate precursor method. *J. Magn. Magn. Mater*. **1999**, *192*, 271-276.

6. Nakamura, T.; Miyamoto, T.; Yamada, Y. Complex permeability spectra of polycrystalline Li–Zn ferrite and application to EM-wave absorber. *J. Magn. Magn. Mater*. **2003**, *256*, 340-347.

7. Waqus, H.; Quresghi, A.H. Influence of pH on nanosized Mn-Zn ferrite synthesized by sol-gel auto combustion process. *J. Therm. Analy. Calori*. **2009**, *98*, 355-360.

8. Rendale, M.K.; Mathad, S.N.; Vijaya, P. Dielectric and magnetic properties of substituted Li-Zn ferrite thick films clouded over a half wavelength microstrip rejection filter. *Int. J. Self-Propag. High-Temp. Synth.* **2016**, *25(2)*, 86–91.

9. Nicolas, J.; Wohlfarth, E.P. Microwave ferrites. In *Ferromagnetic Materials*, Vol. 2; E.P. Wohlfarth, Ed.; North-Holland: Amsterdam, 1980.

10. Baden Fuller, A.J. *Ferrites at Microwave Frequencies*, Peter Peregrinus, London, 1987.

11. Harris, V.G.; Geiler, A.; Chen, Y.; Yoon, S.D.; Wu, M.; Yang, A.; Chen, Z.; He, P.; Parimi, P.V.; Zuo, X.; Patton, C.E.; Abe, M.; Acher, O.; Vittoria, C. Recent advances in processing and applications of microwave ferrites. *J. Magn. Magn. Mater*. **2009**, *321*, 2035-2047.

12. Lagarkov, A.N.; Rozanov, K.N. High-frequency behavior of magnetic composites. *J. Magn. Magn. Mater*. **2009**, *321*, 2082- 2092.

13. Rao, B.P.; Caltun, O.F.; Cho, W.S, Kim, C.-O.; Cheol, G.K. Synthesis and characterization of mixed ferrite nanoparticles. *J. Magn. Magn. Mater*. **2007**, *310*, e812–e814.

14. Kagotani, T.; Kobayashi, R.; Sugimoto, S.; Inomata, K.; Okayama, K.; Akedo, J. Magnetic properties and microwave characteristics of Ni–Zn–Cu ferrite film fabricated by aerosol deposition method. *J. Magn. Magn. Mater*. **2005**, *290–291*, 1442–1445.

15. Xie, J.L.; Han, M.; Chen, L.; Kuang, R.; Deng, L. Microwave-absorbing properties of NiCoZn spinel ferrites. *J. Magn. Magn. Mater*. **2007**, *314*, 37–42.

16. Zhao, H.; Sun, X.; Maoc, C.; Du, J. Preparation and microwave–absorbing properties of NiFe2O4-polystyrene composites. *Physica B* **2009**, *404*, 69-72.

17. Rezlescu, N.; Rezlescu, E.; Tudorache, F.; Popa, P.D. MgCu nanocrystalline ceramic with La^{3+} and Y^{3+} ionic substitutions used as humidity sensor. *J. Opt. Adv. Mater.* **2004**, *6*, 695-698.

18. Chu, X.; Cheng, B.; Hu, J.; Qin, H.; Jiang, M. Semiconducting gas sensor for ethanol based on $LaMgxFe_{1-x}O_3$ nanocrystals. *Sens. Actuators B Chem.* **2008**, *129*, 53-58.

19. Raj, K.; Moskowitz, R.; Casciari, R. Advances in ferrofluid technology. *J. Magn. Magn. Mater*. **1995**, *149*, 174-180.

20. Yattinahalli, S.S., Kapatkar, S.B., Ayachit, N.H.; Mathad, S.N. Synthesis and structural characterization of nanosized nickel ferrite. *Int. J. Self-Propag. High-Temp. Synth.* **2013**, *22(3)*, 147–150.

21. Cannas, C.; Ardu, A.; Peddis, D.; Sangregorio, C.; Piccaluga, G.; Musinu, A. Surfactant-assisted route to fabricate $CoFe_2O_4$ individual nanoparticles and spherical assemblies. *J. Coll. Interf. Sci.* **2010**, *343*, 415-422.

22. Nasr Isfahani, M.J.; Myndyk, M. Magnetic properties of nanostructured MnZn ferrite. *J. Magn. Magn. Mater*. **2009**, *321*, 152–156.

23. Kashid, P.; Mahadev, S.; Kulkarni, A.B.; Mathad, S.N.; Shedam, R. Synthesis and structural studies of nano $Co_{0.85}Cd_{0.15}Fe_2O_4$ ferrite by Co-precipitation Method. *J. Adv. Phys*. **2017**, *6*, 545–548.

24. Zhang, D.; Zhang, X.; Ni, X.; Song, J.; Zheng, H. Low-temperature fabrication of $MnFe_2O_4$ octahedrons: magnetic and electrochemical properties. *Chem. Phys. Lett.* **2006**, *426*, 120–123.

25. Bharamagoudar, R.C.; Angadi, J.; Patil, A.S.; Kankanawadi, L.B.; Mathad, S.N. Structural and dielectrical studies of nano Mn-Zn ferrites prepared by combustion method. *Int. J. Self-Propag. High-Temp. Synth.* 2019 , in press.

26. Clinical and Laboratory Standards Institute. Performance Standards for Antimicrobial Susceptibility Testing; Twenty-Third Informational Supplement CLSI document M100-S23; CLSI: Wayne, PA, USA, 2013.

27. Nalawade, T.M.; Bhat, K.G.; Sogi, S. Antimicrobial activity of endodontic medicaments and vehicles using agar well diffusion method on facultative and obligate anaerobes. *Int. J. Clin. Pediatr. Dent*. **2016**, *9(4)*, 335–341.

28. Rendale, M.K.; Mathad, S.N.; Puri, V. Thick films of magnesium zinc ferrite with lithium substitution: Structural characteristics. *Int. J. Self-Propag. High-Temp. Synth.* **2015**, *24(2)*, 78–84.

29. Thakur, S.; Katyal. S.C.; Singh, M. Structural and magnetic properties of nano nickel–zinc ferrite synthesized by reverse micelle technique. *J. Magn. Magn. Mater*. **2009**, *321(1)*, 1-7.

30. Standley, K.J., *Oxide Magnetic Materials*. Clarendon Press, Oxford, 1972; pp. 11.

31. Jagadeesha Angadi, V.; Rudraswamy, B.; Matteppanavar, S.; Bharathi, P.; Praveena, K. Magnetic properties of nanocrystalline $Mn_{1-x}Zn_xFe_2O_4$. *AIP Conference Proceedings* **2015**, *1665(1)*, 050014.

32. Iravani, S. Bacteria in nanoparticle synthesis. *Int. Sch. Res. Notices* **2014**, Article ID 359316, 18 pages.

33. Prabhu, Y.T.; Rao, K.V.; Kumari, B.S.; Vemula, S.S.K. ; Pavani, T. Synthesis of Fe3O4 nanoparticles and its antibacterial application. *Int. Nano Lett*. **2015**, *5(2)*, 85-92.

34. Wang, L.; Hu, C.; Shao, L. The antimicrobial activity of nanoparticles: present situation and prospects for the future. *Int. J. Nanomed.* **2017**, *12*, 1227-1249.